A simple model to calculate the microstructure evolution in a NiTi SMA

Vittorio Di Cocco

Università di Cassino e del Lazio Meridionale, DICeM, via G. Di Biasio 43, 03043 Cassino (FR), Italy
v.dicocco@unicas.it, https://orcid.org/0000-0002-1668-3729

Stefano Natali

University of Rome "La Sapienza", DICMA, via Eudossiana 18, Roma, Italy
stefano.natali@uniroma1.it, https://orcid.org/0000-0002-2742-0270

ABSTRACT. Shape memory alloys (SMAs) are a wide class of materials characterized by the property to recover the initial shape. This property is due to ability of alloys to change the microstructure from a "parent" microstructure (usually called "Austenite") to a "product" microstructure (usually called "Martensite"). Considering the tensile resistance, SMAs stress strain curves are characterized by a sort of plateau were the transformations from Austenite to Martensite (in loading condition) and from Martensite to Austenite (in unloading condition) take place. In this work a simple model to predict the microstructure modification has been proposed and verified with an equiatomic NiTi alloy characterized by a pseudo-elastic behavior.

KEYWORDS. Shape memory alloy; Austenite; Martensite; Microstructure transitions.

INTRODUCTION

Shape memory alloys (SMAs) are an interesting class of materials which is usually employed in many fields of the aerospace and civil industry. Thanks to the high resistance against corrosion in many aggressive environments, SMAs are also used in medicine for construction of prosthesis [1, 2]. In the last years, the use of SMAs in electric field is more and more increased, especially in piezoelectric and in self-healing devices. In the last decades, several investigations have been carried out in order to characterize such alloys and take advantage of their peculiar properties in different applications [3-7].

In particular, SMAs are able to recover the original shape, even after severe deformations. The explanation of this peculiar behavior is due to both crystallography and thermodynamic properties of SMAs which allow a reversible phase transition from the parent phase (austenite) to the product phase (martensite) [8-13]. Note that the twinning deformation mode characterizes the above transition. This is a reversible deformation process and differs from other irreversible processes, such as the slip deformation mode [9, 11].

It is important to underline that SMAs deformations can be recovered as follows [7-9]:

1) Shape memory effect, where the recovery of initial shape depends on the material heating up to a critical temperature;
2) Pseudoelastic effect, where the recovery of initial shape is due to the unloading process, being the critical temperature lower than the environment temperature.

The microstructure transformation takes place at the material strain threshold up to this deformation level, the stress-strain behavior is linear with the austenite Young modulus. Over this strain value, the transformation of austenite in martensite takes place, and the stress-strain behavior is quite similar to a plateau. When the transformation of austenite to martensite is completed, the stress-strain behavior becomes linear according to the Young modulus of martensite.

In this work, the austenite and martensite volume fractions were measured using XRD analyses for different imposed strains both in loading and in unloading conditions. Furthermore, the influence of cycling was analyzed and a simple model able to calculate the microstructure quantities was proposed.

INVESTIGATED ALLOY AND METHODS

I n this work, an equiatomic NiTi shape memory alloy, characterized by a pseudoelastic behavior, is investigated. The alloy was obtained by using a vacuum furnace where a crucible made of ittria was charged using pure Ni and pure Ti powders. The cast was obtained from melted alloy using centrifugal force obtained by high crucible rotation. The melting was cooled in a graphite casting molds in rectangular mini-ingots (40x30x10 mm).

From the casting ingots, flat tensile specimens characterized by the shape in Fig. 1 were obtained by electrical discard machining (EDM).
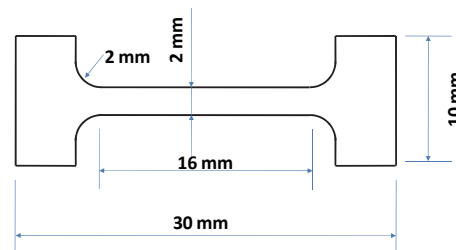

Figure 1: Mini dog-bone tensile specimens: thickness 1 mm.

Tests were performed by means of patented mini-tensile machine that is characterizes by a removing frame (Fig. 2) able to keep the specimens under scheduled deformation in order to analyze the microstructure.
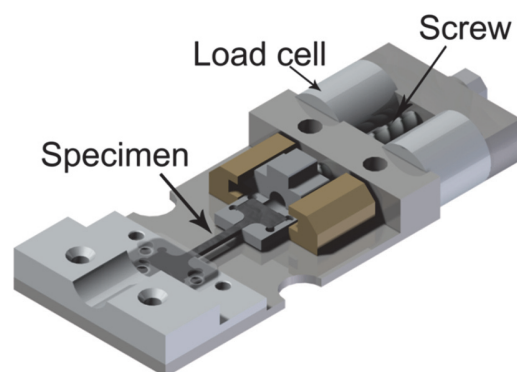

Figure 2: Removing frame of tensile minimachine.

Diffractions measurements were performed step by step corresponding to 1, 10, 50 and 100 cycles both in loading and in unloading conditions. For each investigated loading step, the loading frame containing the specimen was removed from the testing machine, at fixed values of deformation. The specimens, under load condition, were analyzed using a diffractometer to evaluate XRD spectra. XRD measurements were performed using a Philips X-PERT diffractometer equipped with a vertical Bragg–Brentano powder goniometer. A step–scan mode was used in the 2θ range from 40° to

90° with a step width of 0.02° and a counting time of 2 s per step. The employed radiation was monochromated CuKα (40 kV – 40 mA). The investigated steps are loading and unloading conditions. The analyzed diffraction steps conditions are shown in Tab. 1.

$\varepsilon_{eng.}$ in loading conditions [%]	$\varepsilon_{eng.}$ in unloading conditions [%]
0.00	---
2.50	9.15
3.33	8.32
4.16	7.49
5.00	6.66
5.83	5.83
6.66	5.00
7.49	4.16
8.32	3.33
9.15	2.50
10.00	0.00

Table 1: XRD analyzed deformations steps in loading and in unloading condition a 1 and 50 cycles.

RESULTS AND DISCUSSION

X-Ray diffractions spectra

Considering the equiatomic NiTi investigated alloy, the diffraction spectrum of the initial unloaded specimen is shown in Fig. 3 (Cycle 1, ε = 0%). In this spectrum the main peak is measured corresponding to 2θ=42.27° and a secondary peak is measured at 2θ=43.21°.
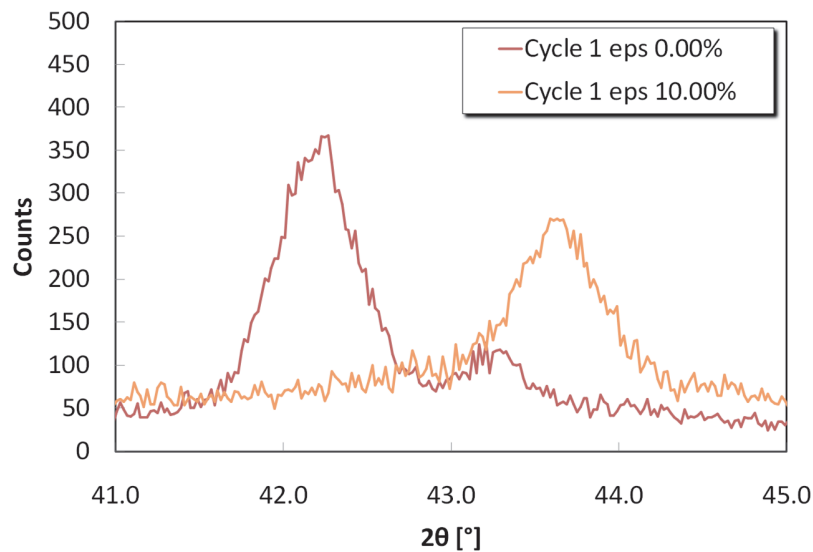

Figure 3: Diffraction spectra of equiatomic NiTi at ε_{eng}=0% and at ε_{eng}=10% for the first cycle: peaks of Austenite (corresponding to ε_{eng}=0%) and Martensite (corresponding to ε_{eng}=10%)

These peaks correspond to the austenite phase, and no evidence of a different microstructure is shown in the spectrum in the analyzed angles range. The spectrum corresponding to higher deformation value (ε_{eng}=10%) shows the presence of a single peak in the investigated range (Fig. 3 - Cycle 1, ε = 10.00%). This peak corresponds to a fully martensitic structure. Both spectra imply a microstructure modification from a fully austenitic to a fully martensitic one due to the effect of deformation.

Removing the imposed deformations, the initial shape is completely recovered, and the spectrum obtained in unloading conditions (Fig. 4 – Cycle 1, ε =0.00% - Unloading) is similar to the initial spectrum (Fig. 3 – Cycle 1 eps 0.00%). This result implies that the microstructure is fully changed from martensite to austenite phase. This behavior corresponds to a pseudoelastic SMA behavior, and the differences between the spectra in Fig. 4 are due to the damage generated by the first loading-unloading cycle as already observed in Di Cocco et al. [12].

As shown in Fig. 5, the spectra obtained after 50 cycles are different from to the spectra obtained after 1 cycle (Fig. 3). However the ability to recover the initial austenitic structure is not compromised as shown on Fig. 6, where the spectrum obtained at ε_{eng}=0.00% is quite similar to the spectrum obtained in unloading condition at ε_{eng}=0.00% (after 50 cycles).

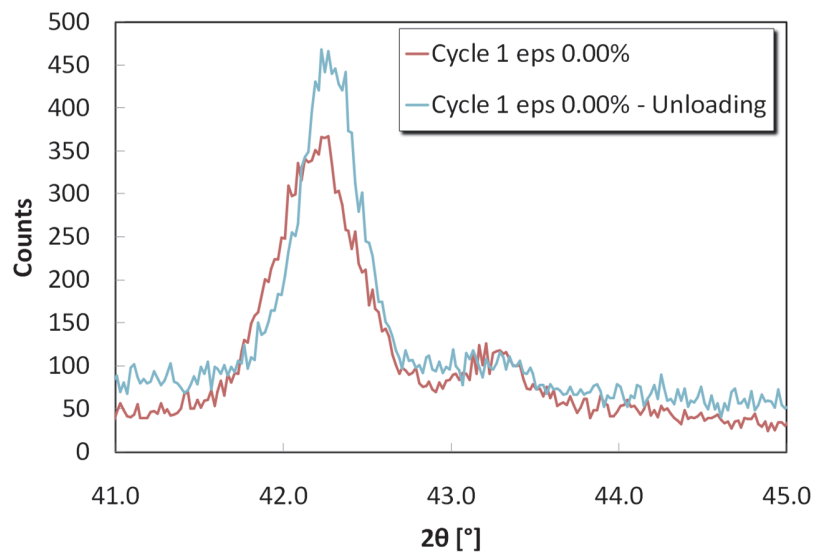

Figure 4: Diffraction spectra of equiatomic NiTi at ε_{eng}=0% both before and after the first cycle.
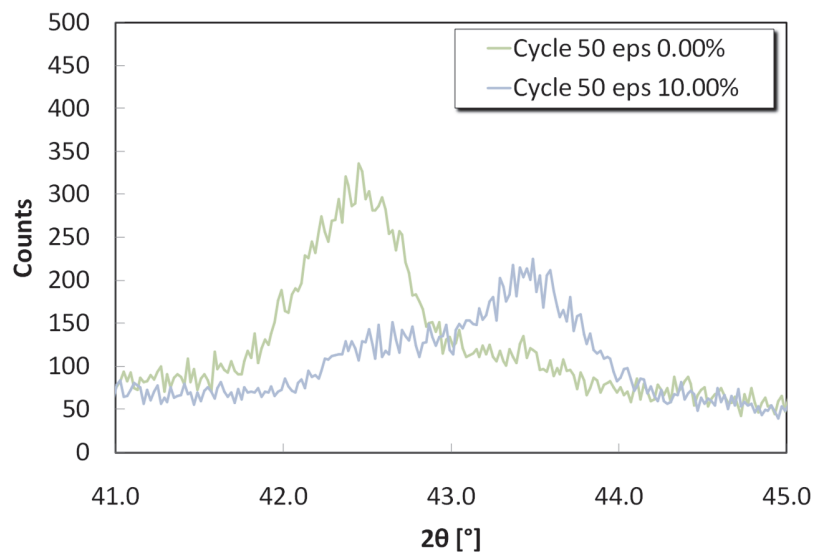

Figure 5: Comparison between spectra obtained for at cycle 50: at ε_{eng}=0.00% and ε_{eng}=10.00%
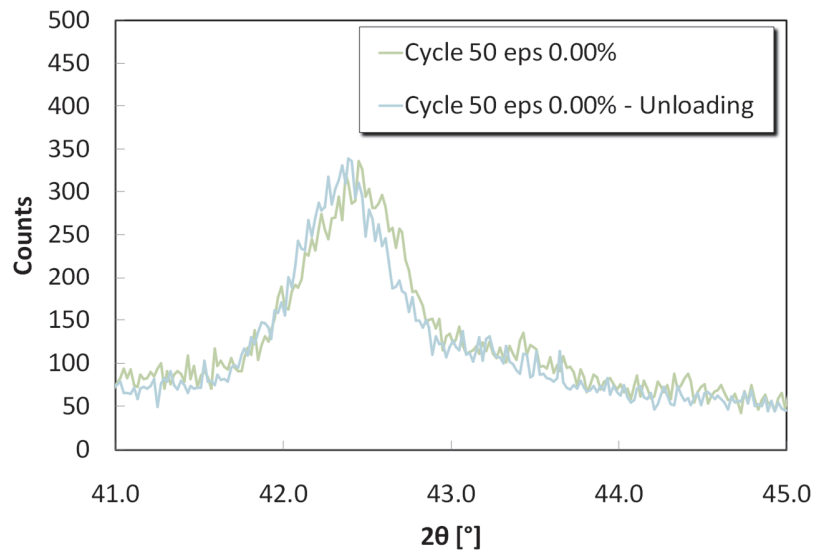
Figure 6: Comparison between spectra obtained for at cycle 50 at ε_{eng}=0.00% both in loading and in unloading conditions.

Differences in diffraction spectra are not only due to the cycling damage of the investigated alloy but are also due to the hysteresis as shown in Fig. 7, where the spectrum corresponding to ε_{eng}=6.66% in loading condition is compared to the spectrum obtained at same strain in unloading condition. The presence of different mean peaks implies that the hysteresis phenomenon allows two different microstructure equilibrium conditions (under loading and unloading conditions, respectively).
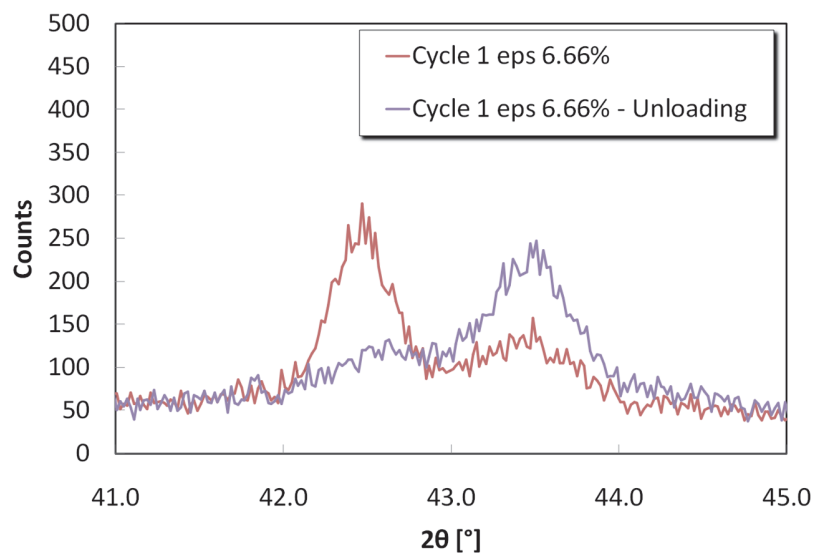

Figure 7: Comparison between spectra obtained for the first cycle at ε_{eng}=6.66% both in loading and in unloading conditions.

Microstructure evaluation
Considering all the spectra obtained in the XRD analyses for each investigated condition (Tab. 1), the quantification of microstructure is performed by means of measure of amplitude of main austenite and martensite peaks. In order to evaluate the amplitude of main peaks, a ground signal is subtracted from the measure of each peak. The ground values are obtained from the spectrum at ε_{eng}=0.00% for the martensite and from the spectrum obtained at ε_{eng}=10.00% for the austenite. Both the quantification of austenite and the martensite are obtained normalizing to 1 the amplitude of corresponding mean peaks. In addition, considering that only two phases were observed (austenite and/or martensite), the measure of microstructure contents is assumed as complement to 1 to the structure characterized by a peak better identified in XRD analysis.

As an example, results of structure quantifications, in terms of volumetric quantification, are shown in Fig 8 for the first cycle and in Fig. 9 for the cycle 50.
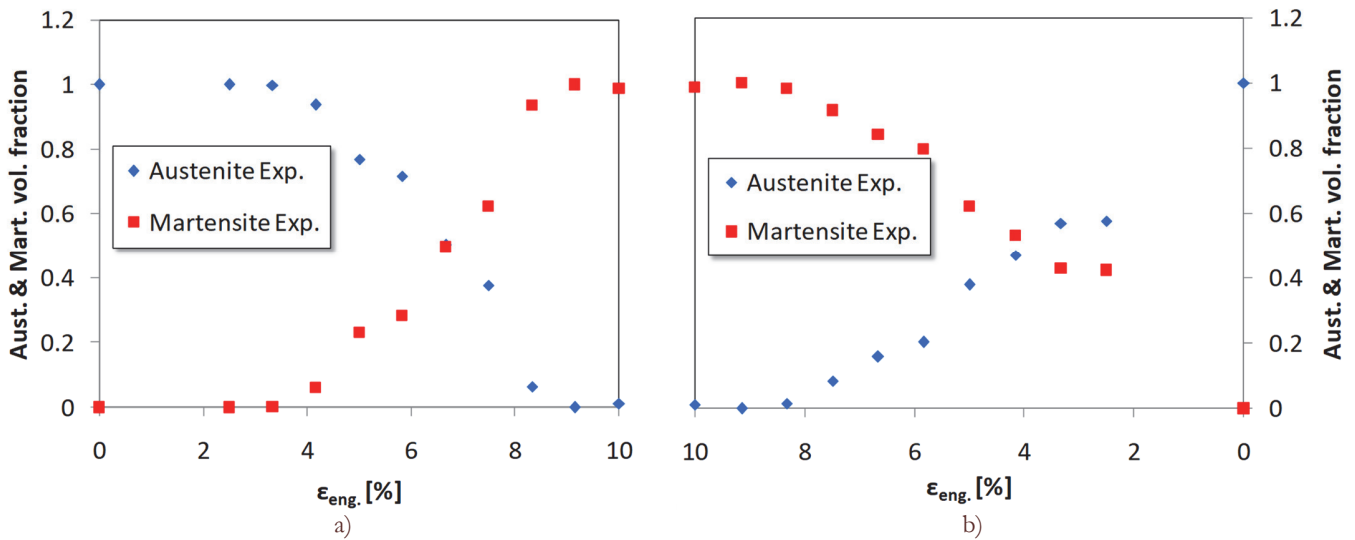

Figure 8: Quantification of microstructure corresponding to the first cycle: a) loading condition, b) unloading condition.
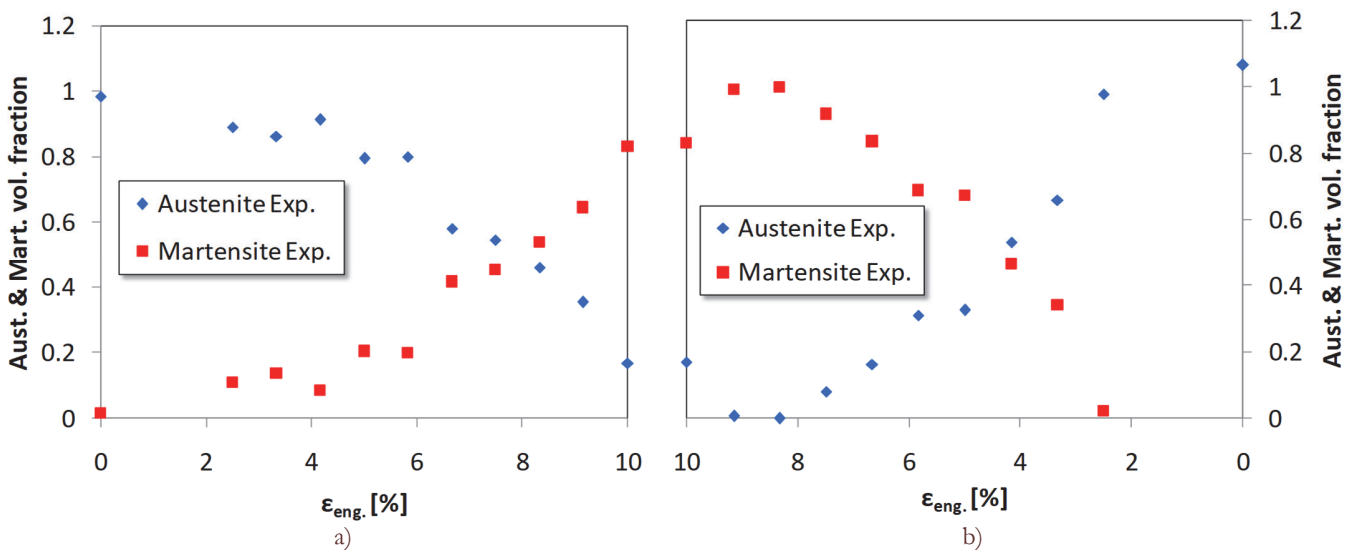

Figure 9: Quantification of microstructure corresponding to the cycle 50: a) loading condition, b) unloading condition.

Microstructure prediction model

In this work, a function E is assumed to be associated to microstructural changing in SMAs alloys (Eq. 1). This function depends on the engineering strain ε and by the austenite A or martensite M volume fractions (normalized to 1).

$$E\left(\varepsilon, A, M\right) \tag{1}$$

The infinitesimal variation of Eq. 1 is due to three different contributions:

1) The first one is the contribution of imposed strain and it is assumed in proportional form using a constant C which depends on materials and their conditions (e.g. damage, cycling, and so on);

2) The second one is the variation of Austenite (Austenite volume fraction);
3) The third contribution is the variation of Martensite (Martensite volume fraction).

In the loading conditions the microstructure transition is from Austenite to Martensite; for this reason, the contribution of austenite variation is assumed as positive and the contribution of Martensite variation is assumed negative as shown in Eq. (2)

$$dE(\varepsilon, A, M) = Cd\varepsilon + \frac{dA}{A} - \frac{dM}{M} \tag{2}$$

To evaluate the equilibrium conditions of structure the differential form of Eq.2 is imposed to zero as shown in Eq. 3. The integration of Eq. 3 is shown in Eq. 4, and the integrated form is shown in Eq. 5.

$$dE = Cd\varepsilon + \frac{dA}{A} - \frac{dM}{M} = 0 \tag{3}$$

$$\int Cd\varepsilon + \int \frac{dA}{A} - \int \frac{dM}{M} = D \tag{4}$$

$$D = C\varepsilon + lnA - lnM = C\varepsilon + ln\frac{A}{M} \tag{5}$$

Expliciting Eq. 5 in terms of A/M ratio (Eq. 6) and considering the volume fraction of the Austenite as a complement to 1 of Martensite volume fraction (under the hypothesis of presence of only austenite and martensite without any other phases) the Austenite/Martensite ratio can be expressed by Eq. 7.

$$ln\frac{A}{M} = D - C\varepsilon \rightarrow \frac{A}{M} = e^{D-C\varepsilon} = De^{-C\varepsilon} \tag{6}$$

$$\frac{1-M}{M} = De^{-C\varepsilon} \tag{7}$$

From Eq. 7 is trivial to evaluate the content of Martensite (Eq. 8) and of Austenite (Eq. 9)

$$M = \frac{1}{1 + De^{-C\varepsilon}} \tag{8}$$

$$A = 1 - M = 1 - \frac{1}{1 + De^{-C\varepsilon}} = \frac{De^{-C\varepsilon}}{1 + De^{-C\varepsilon}} \tag{9}$$

The evaluation of parameters C and D is obtained by minimizing square errors of values obtained from Eq. 8 and Eq. 9 and the experimental microstructure quantifications. For example in Fig. 10 the results obtained by Eq. 8 and 9 are plotted whit the corresponding experimental results shown in Figs. 8 and 9.

Considering all the investigated cycles (1, 10, 50 and 100) the evaluation of C and D parameters are shown in table 2, where the parameter D can assume only two values (700 in loading conditions and 70 in unloading conditions). This parameter indicates the hysteresis phenomena of the microstructure transition and it doesn't depend on the cycles.

The effect of the cycles is taken into account by the parameter C, which is influenced by the cumulative cyclic damage. Plotting the parameter C as a function of loading cycles in a bi-logarithmic plane, a linear correlation is obtained (Fig. 11). More evident differences of the C parameter are observed corresponding to low cycles (between 1 and 10 cycles) where the main damages are observed [12, 13].
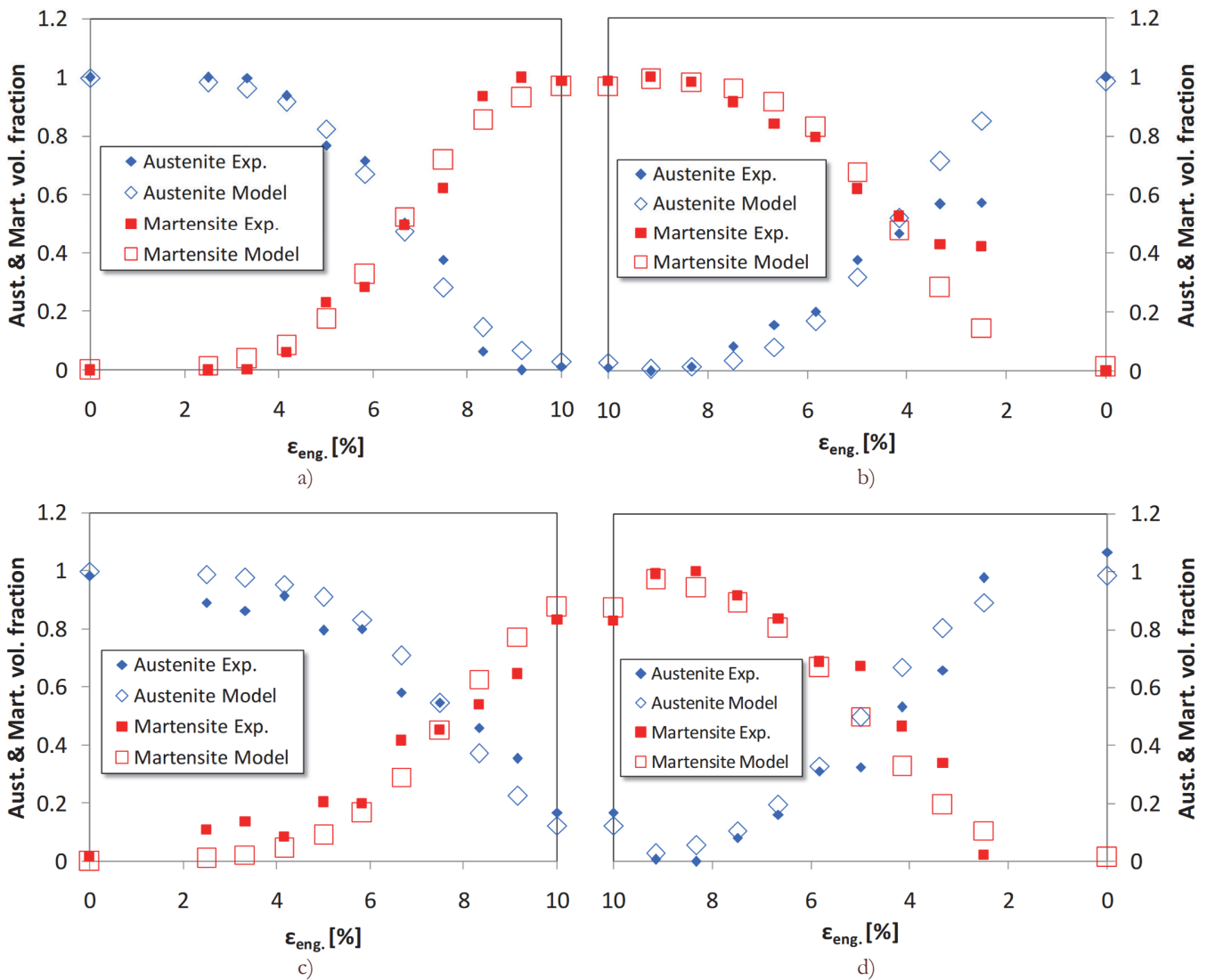
Figure 10: Comparison of microstructure quantifications: a) cycle 1 loading conditions, b) cycle 1 unloading condition, c) cycle 50 loading condition, d) cycle 50 unloading condition.

Cycle	C	D Loading/Unloading
1	1	700/70
10	0.9	700/70
50	0.85	700/70
100	0.8	700/70

Table 2: Evaluation of C and D parameters.

CONCLUSION

In this work, the microstructure modification of a pseudoelastic equiatomic NiTi alloy was investigated by means of XRD diffraction on tensile dog-bone specimens using a non standard mini-tensile machine. Following this procedure, it was possible to obtain the diffraction spectra under imposed deformations. The measured spectra were

elaborated to evaluate the austenite and martensite volume fractions for each investigated deformation value (both in loading and in unloading conditions). The analyses were performed after 1, 10, 50 and 100 loading cycles.

The results of experimental quantification of austenite and martensite volume fractions showed a non linear modification of the microstructure due to imposed strain and the influence of hysteresis.

A simple model was proposed in order to calculate the austenite and martensite volume fractions at different imposed strains both in loading and in unloading conditions. The model takes into account both the hysteresis phenomenon and the cycling damage of material by using two parameters:

1) The parameter C (it takes into account the damage due to the cyclic loading);
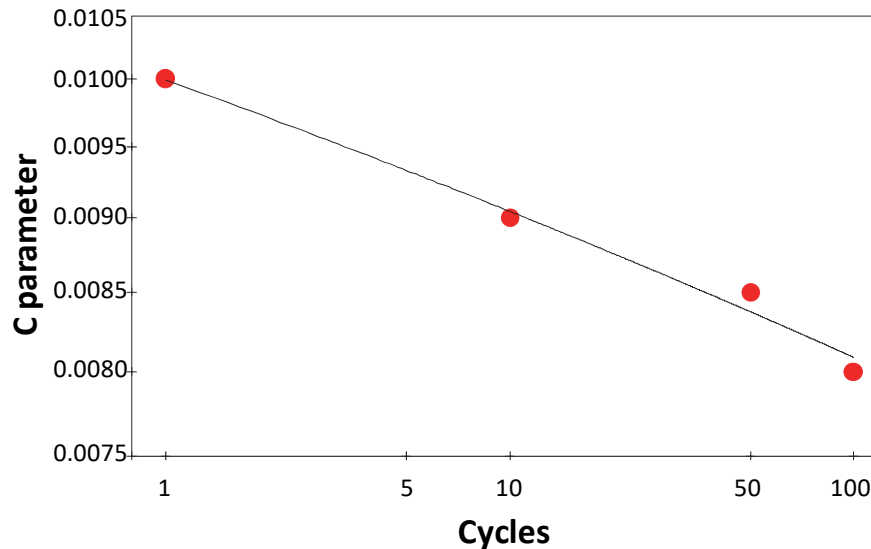2) The parameter D (it takes into account the hysteresis).

Figure 11: Influence of cycling on C parameter.

REFERENCES

[1] Bogue, R. (2014). Smart materials: A review of capabilities and applications, Assembly Automation., 34, pp. 16-22.
[2] Ogai, H. and Bhattacharya, B. (2018). Introduction to Smart Materials, Intelligent Systems, Control and Automation., Science and Engineering, 89, pp. 123-151.
[3] Amariei, D., Frunzaverde, D., Vela, I. and Gillich, G.R. (2010). Educational stand using shape memory alloys to enhance teaching of smart materials., Procedia Social and Behavioral Sciences, 2, pp. 5104-5108.
[4] Lemmens, R.J., Dai, Q. and Meng, D.D. (2014). Side-groove influenced parameters for determining fracture toughness of self-healing composites using a tapered double cantilever beam specimen., Theoretical and Applied Fracture Mechanics, 74, pp. 23–29.
[5] Bhargava, RR. And Verma, P.R. (2016). Strip-electro-mechanical yield model for transversely situated two semi-permeable collinear cracks in piezoelectric strip., Theoretical and Applied Fracture Mechanics, 81, pp. 32–49.
[6] Hu, K., and Chen, Z. (2016). Boundary effect on crack kinking in a piezoelectric strip with a central crack., Theoretical and Applied Fracture Mechanics, 81, pp. 11–24.
[7] Oudah, F. and El-Hacha, R. (2017). Joint performance in concrete beam-column connections reinforced using SMA smart material., Engineering Structures 151, pp. 745–760.
[8] Shaw, J.A. and Kyriakides, S. (1995). Thermomechanical aspects of NiTi., Journal of the Mechanics and Physics of Solids 43(8), pp. 1243-1281.
[9] Otsuka, K. and Ren, X. (1999). Recent developments in the research of shape memory alloys., Intermetallics, 7 pp. 511-528.
[10] Liang, W., Zhou, M. and Ke, F. (2005). Shape Memory Effect in Cu Nanowires., Nano Letters, 5(10), pp. 2039-2043.
[11] Otsuka, K. and Ren, X. (2005). Physical metallurgy of Ti–Ni-based shape memory alloys., Progress in Materials Science, 50, pp. 511–678.

[12] Di Cocco, V., Iacoviello, F., Maletta, C. and Natali S. (2014). Cyclic microstructural transitions and fracture micromechanisms in a near equiatomic NiTi alloy., International Journal of Fatigue, 58, pp. 136–143. http://dx.doi.org/10.1016/j.ijfatigue.2013.03.009

[13] Di Cocco, V., Vantadori, S., Carpinteri, A., Iacoviello, F. and Natali, S. (2018). Fatigue Analysis of a near-equiatomic pseudo-elastic NiTi SMA., Theoretical and Applied Fracture Mechanics, 94, pp. 110-119. https://doi.org/10.1016/j.tafmec.2018.01.012.